PROGRESS REPORT

DIRECTIONAL DOPPLER BLOODFLOW METER

NRG 33-010-074

to

National Aeronautics & Space Administration

by

F. D. McLeod

Dept. of Physiology

Cornell University

Grant NRG 33-010-074 May 1969

INTRODUCTION

The pattern of oscillatory flow observed in the arterial system is dependent upon cardiac function, as well as the location of the artery, its size, the resistance of the bed its supplies, and the physiological conditions under which the observations are made.[1] The flow curve recorded from a major artery supplying the vascular beds of relatively high resistance consists of a large systolic forward flow component which is immediately followed by a brief period of flow reversal. A second small forward flow component may occur prior to the next pulse cycle. In regions of low vascular resistance such as the brain, liver, and kidneys, there is usually a much larger mean flow component without flow reversal.

The need for accurate measurement of the directional components of arterial and venous flow has been obvious to the physiologist who is interested in describing the physical behavior and characteristics of the circulatory system. The demand or need for similar information in clinical medicine has not been as apparent except as it relates to the determination of average cardiac output. Information relative to the oscillatory flow pattern has been recorded in animals with the electromagnetic flowmeter which permits recording of instantaneous velocity and flow direction. Although the electromagnetic flowmeter has been extensively applied in animal studies, its utility is limited by uncertain baseline shifts and the difficulty of obtaining meaningful in vitro calibrations. Application in man is further limited because it requires: (1) surgical exposure of the vessel; (2) it is not easily used on veins; and (3) the required anesthesia, depending on type and conditions, may profoundly influence

cardiovascular dynamics.

Interest in the prospect of measuring both instantaneous velocity and flow was stimulated by observations made with the Doppler ultrasonic blood flowmeter.[2,3] The instrument utilizes the Doppler shift experienced by high frequency ultra sound scattered off of moving blood cells to provide transcutaneous, observations as well as catheter tip and implanted probe studies. Sample Doppler instruments, while providing information relative to flow velocity, cannot differentiate between the positive and negative Doppler shifts produced by forward or reverse velocity components. A positive output is produced by both forward and reverse velocity. Sine-wave and oscillatory flows thus appear to be full wave rectified. Unfortunately, many physiological flows are oscillatory thereby sharply limiting the potential broad application of the instrument.

A phase detection technique, first used in single sideband communications equipment[4] and more recently in laser interferometry,[5] has been adapted for identification and separation of Doppler shifts produced by positive and negative velocity components. The method[6] utilizes two detectors, operating in quadrature, to identify the signals phase rotation, and thus the direction of flow. The method retains the inherent zero reference and linearity of the simpler non-directional Doppler flowmeter.

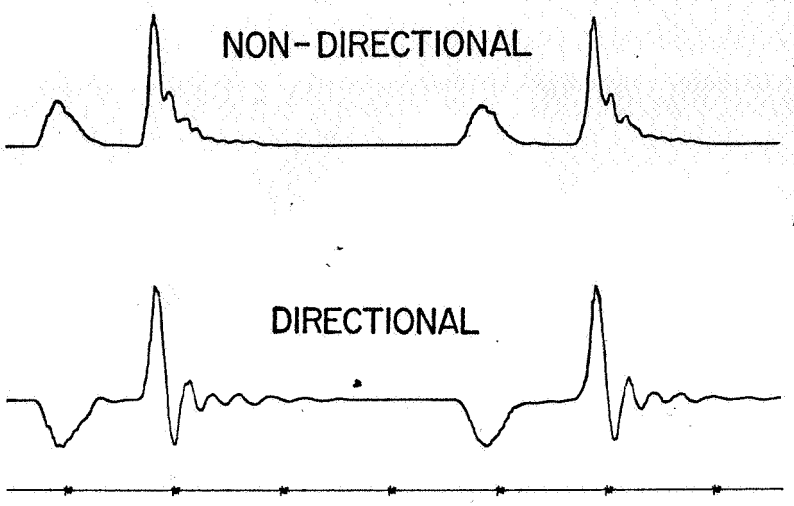

Figure 1. Stop flow transient showing full wave reclificiation of damped oscillatory flow by non-directional flowmeter. It is impossible to tell that the flow has gone through zero on the non-directional trace.

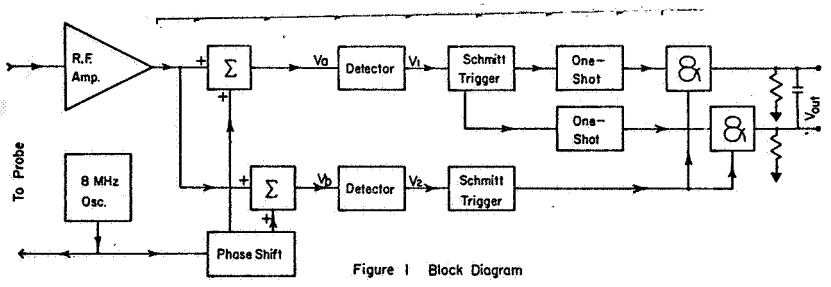

Figure 1 Block Diagram

Figure 2. Block diagram of the directional Doppler flowmeter

METHODS

Basic Principle

Blood cells provide sufficient interface to scatter and reflect a small portion of an incident beam of high frequency (7-11 M Hz) ultra sound. The frequency of waves scattered from stationary interfaces is the same as that of the incident wave; however, waves scattered from moving particles experience a frequency shift proportional to the scattering cell's velocity. The frequency shift, described by the Doppler equation, is:

$$F_d = 2 F_c \frac{2 \cos \alpha}{C} \qquad \text{Eq. 1}$$

where: F_d = frequency shift or difference frequency.

F_c = frequency of incident wave.

V = vector component of scattering particles velocity along an axis bisecting the angle between the transducer elements

α = half angle between transducer elements.

C = velocity of sound in fluid.

For a typical physiological application: F_c = 10 MHz; C = 1.4 x 10^3 M/sec; $\alpha = 45^o$; V ranges from 0 to $\pm$ 1 m/sec; the Doppler shift ranges from 0 to 10 KHz.

The blood stream consists of a large number of random scatters moving in a velocity profile. The scattered signal is not a descrete frequency but a power spectrum representative of the flow profile. The reflected signal is expressed as

$$P(f_d) = A\ (v)$$

where A(v) is the vessel crossectional area occupied by fluid moving at velocity V. The large number of random on Gaussian scatters permits expression of the mean velocity as the first moment of the power spectrum $[P(f_d)]$*.

The power received at the second or receiving piezoelectric transducer is amplified and demodulated so as to preserve both amplitude and phase information. The demodulation process shown in figure 2 translates the scattered power spectrum to the origin where the direct coupled carrier appears as a zero frequency of D.C. component and is easily removed with a blocking capacitor. An empirical zero crossing technique is used to produce a voltage output proportional to the first moment of the demodulated power spectrum.

*A field of coherent or organized scatters would have implied use of the first moment of the voltage spectrum.

Transducer signal

Two piezoelectric transducers are placed adjacent to the artery (fig. 3). One transducer, excited in the thickness mode, directs a beam of 10 MHz. ultrasound into the flow stream, while the other transducer serves as a receiving element for the waves scattered from the moving cells. A conversion and coupling loss of 15 db is observed for the LTZ-5* transducer material. Both the exciter and scattered sound experience an attenuation in tissue of approximately 10 dB/CM at this frequency.

The maximum possible scattered signal can be estimated by attributing all losses in this frequency range to scattering. A 1 cm scattering path attenuates the exciter or incident beam approximately 10 dB or 90%. The power available for scattering, and thus the maximum amounts of scattered signal one can expect, is in the order of -0.5 dB. A 4 mm. diameter receiving transducer placed 1 cm from the scatterer intercepts approximately 1% (-20 dB) of the isotropically scattered sound. The scattered signal appearing at the terminals of the receiving transducer is exciter signal minus all attenuation, scattering, and insertion losses. At the very best, the received signal is 70 dB down from the exciter input. This approximation represents the maximum possible signal. Unfortunately, most arteries are smaller than 1 cm and deeper than 1 cm; a more typical signal can be as much as 80 or 90 dB down.

Electrical leakage and acoustic coupling are responsible for

*Transducer Products, Torrington, Connecticut

direct coupling a portion of the exciter power into the receiving transducer. The worst-case acoustic-coupled signal can be approximated as the combined insertion loss of the two transducers, in this case 30 dB. Electrical leakage is estimated by assuming a voltage division between the leakage path and transducer impedances. Typical impedance values of; 10^4 ohms leakage and 10^2 ohms transducer yield a direct coupling of -40 dB. Electrical insulation can be used to reduce this leakage component, however it is of little value as the larger acoustic signal cannot be avoided.

In summary, the received signal, shown in figure 4, consists of a leakage carrier component approximately 30 dB. down from the exciter and a Doppler shifted power spectrum 20 KHz wide and between 70 and 90 dB. down from the exciter.

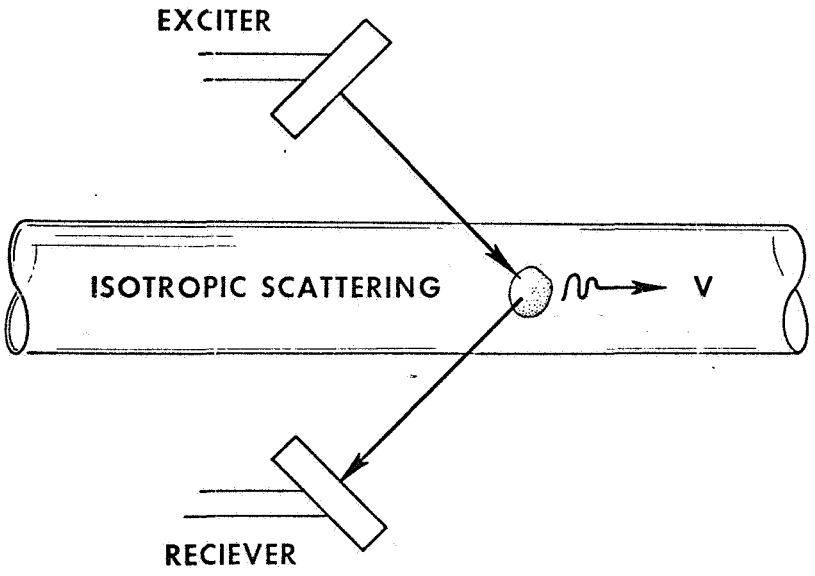

Figure 3. Schematic diagram illustrating placement of transducer elements. Angle α is measured from the flow axis to the center of the sound beam.

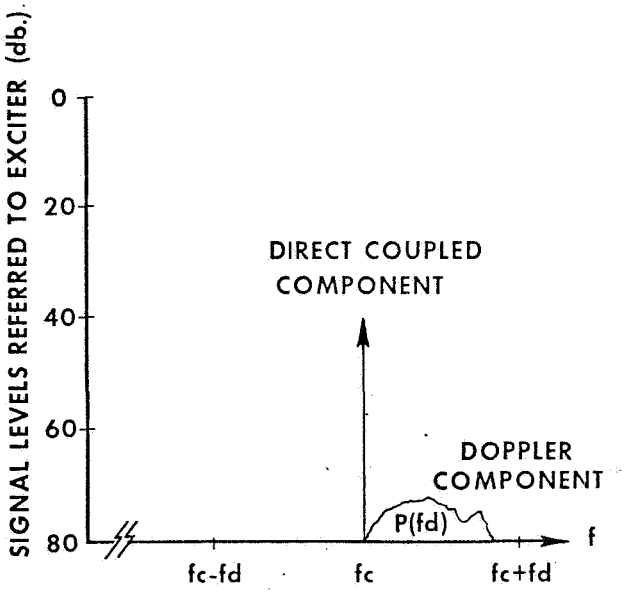

Figure 4. The relationship between exicter and predicted received power levels. The received levels shown represent a best case approximation, typical signals can be as much as 80 or 90 db. down from the exicter power level.

System Considerations

A good signal to noise ratio is required if we are to accurately compute volume flow and mean velocity as the first moment of the power spectrum. As seen in figure 5, noise effectively alters the calibration factor $\frac{2}{}$. Taking ± 1% as the minimum acceptable accuracy, a 20 dB. signal to noise ratio is required. Assuming demodulator input noise as 1 μV RMS it is possible to determine the following system parameters.

a) Received input signal level:

$$V_d > 20 \text{ dB. } V_n$$

$$> 10 \times 1\mu \text{ V}$$

$$> 10\mu \text{ V RMS}$$

b) Exciter Power Level:

$$Ve \simeq (70 \rightarrow 90) \text{ dB } 10 \text{ V}$$

Taking the worse Case:

$$Ve \simeq 90 \text{ dB } 10 \mu V$$

$$\simeq 10\mu \text{ V} \times 10^4 \times \sqrt{10}$$

$$\simeq .3 \text{ V RMS}$$

c) Leakage Component:

$$V_1 = (-30 \text{ dB.}) V_e$$

$$= .3X (-30 \text{ Db.})$$

$$= 10 \text{ MV RMS}$$

These system parameters are intended only as design guides and are not based upon a rigorous development.

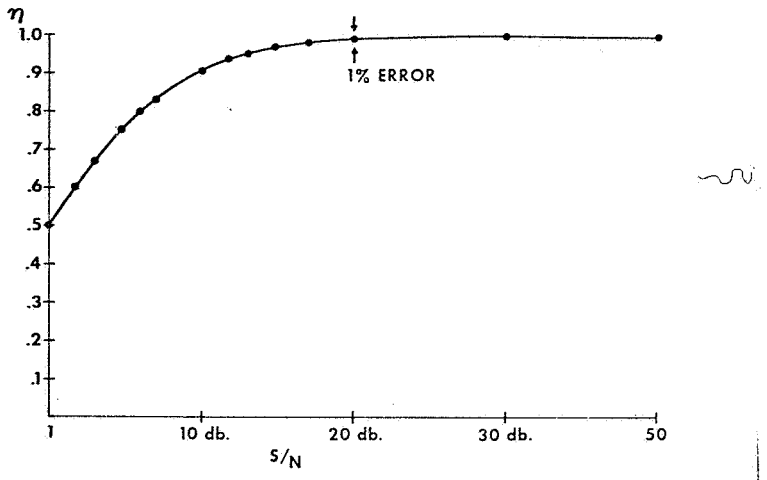

Figure 5a. The relationship of signal to noise ratio and calibration factor. A curve of the form $S/N / S/N+1$ results from superimposing the reciever signal power spectrum on a band limited white noise spectrum. A 20 db S/N ratio is required for ± 1% accuracy.

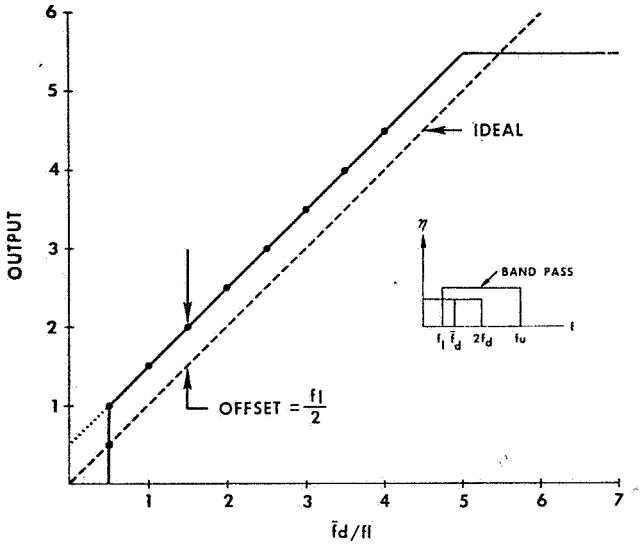

Figure 5b. The effect of band limiting on linearity and calibration. Removal of low frequency components introduces a zero offset $f_L/2$ Elimination of high frequencies limits the maximum measurable velocity.

BANDPASS CONSIDERATIONS

The power distribution of the Doppler shifted signal is largely determined by the velocity profile. If the Doppler signal is to be properly interpreted in terms of velocity profile and mean flow on adequate bandpass must be provided to preserve the amplitude and frequency content of the signal. An insufficient low frequency response will tend to ignore the low frequency shifts produced by the slow moving blood the outer portions of the profile, placing undue emphasis on the higher velocity components. Cutting off or bypassing high frequency components limits the maximum velocity and tends to flatten the peaks of cardiac waveforms. Such limiting can completely mask diagnosis of diseases such as aortic and mitral stenosis. Selection of the system bandpass represents a compromise between preserving the integrity of signal and eliminating the noise and motion artifactis by limiting the bandpass.

The average velocity determined as the centroid of the power spectrum is;

$$\bar{f} = \frac{\int f P(f)\, df}{\int P(f)\, df}$$

After bandpassing the power spectrum becomes,

$$P(f)_L = P(f)\, F^2(f)$$

where: $F(f)$ is the system transfer function.

Substituting, the centroid of the band limited power spectrum becomes:

$$\bar{f}_\cdot = \frac{\int F^2 f\, P(f)\, df}{\int F^2 P(f)\, df}$$

Evaluation of this expression is possible by assuming:

a. A rectangular power spectrum

b. A rectangular bandpass such that F(f) = 1 over the bandpass a F(f) = 0 above and below the cutoff points f_l and f_u.

The mean velocity becomes

$$\bar{f}_c = \frac{\int_{f_l}^{f_u} f\,P(f)\,df}{\int_{f_l}^{f_u} P(f)\,df}$$

Thus, the introduction of a rectangular bandpass places finite limits, fz and fu, on the centroid integral. Figure 5b illustrates the bounding of a rectangular power spectrum. The resulting calibration curve is displaced or offset by an amount $f_z/_2$ and limited at fu. Unfortunately, this zero offset cannot be corrected by simple base line suppression as forward and reverse velocities are shifted in opposite directions. A 100 Hz low frequency cutoff represents a reasonable compromise between zero offset and wall motion artifacts. The velocity error introduced to a 10MHz. Doppler flowmeter is in order of 5mm/sec or approximately 7 ml/min in a 5 mm diameter vessel. A 15 KHz upper band limit is adequate for most Doppler shifts which generally range up to 11 KHz. This limits the peak mean velocity at 3/4 M/sec or 1 liter/min in a 5 mm vessel.

EXCITER

A Colpitts oscillator and driver amplifier provides R. F. excitation to the transucer. The circuit, shown in Figure 8a, developes 1 volt RMS across the piezoelectric emmitter element. The LTZ-5 transducer elements have a resonant impedance of approximately 50 ohms. The accoustic power generated is less than 20 mw/cm^2. A 15 db. isertion loss results from the impedance miss-match between the transducer element and tissue. Less than 1 mw/cm^2 acoustic energy is actually coupled into the tissue. Exciter power consumption is 60 mw over the 7-10 MHz tuning range.

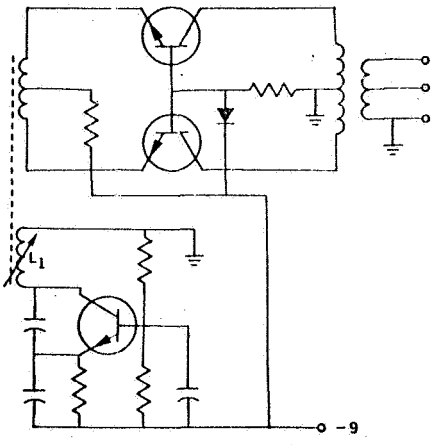

Figure 8a. Exciter oscillator and driver amplifier.

Frequency is adjusted to the transducer resonant frequency by an adjustable core in inductance L_1.

Demodulation

The presence of the large carrier or leakage component rules out the use of conventional FM demodulation techniques. Both ratio and Foster-Seely detectors tend to capture on the larger carrier component, ignoring the smaller Doppler shifted signal. Simple diode, or square-law detection, as used in earlier Doppler instruments, recovers only amplitude and absolute frequency information; positive and negative Doppler shifts cannot be differentiated. This limitation makes the instrument unable to distinguish between forward and reverse flows. An oscillatory flow signal appears to be full wave rectified.

A phase detection technique,[4] used in single-sideband and other communication systems,[5] has been adapted to recover both amplitude and phase information. The process introduces a phase shift prior to detection that after detection retains the sign of the frequency shift. Phase Shift δ is produced by addition of carrier components, large compared to the leakage component. Two separate detectors are used to provide a reference from which δ is measured.

The lead-lag relationship of the detector outputs is determined solely by the sign of the Doppler shift, making the method free from zero drift.

Referring to the phasor diagram, Fig. 6, components of the form; A cos $(W_c t + \frac{\pi}{4})$ and A cos $(W_c t - \frac{\pi}{4})$ are separately added to the input signal to obtain

$$V_a = F\cos(\omega_c t + \beta) + D\cos(\omega_c + \omega_d)t$$

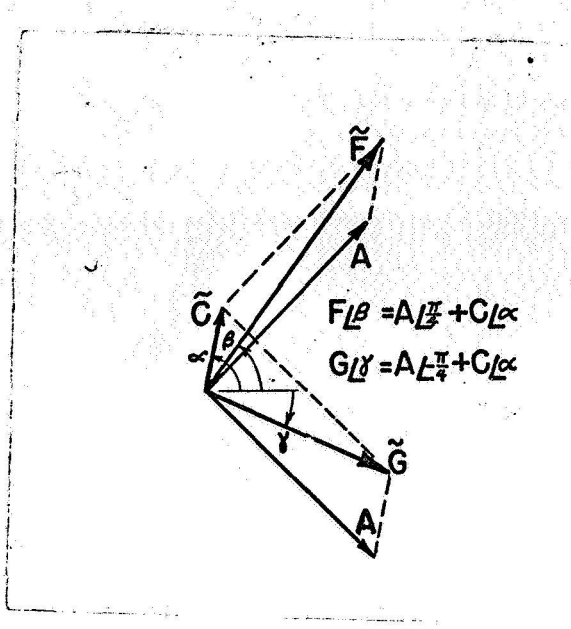

Figure 6. Phaser diagram. Two quadature components are added to the received signal to produce phase between the carrier inputs to the mixers. Angle α is included to allow for random variation of the direct coupled component phase and the added components. In order to maintain the sence of the added components should always be greater than approximately twice the direct coupled component.

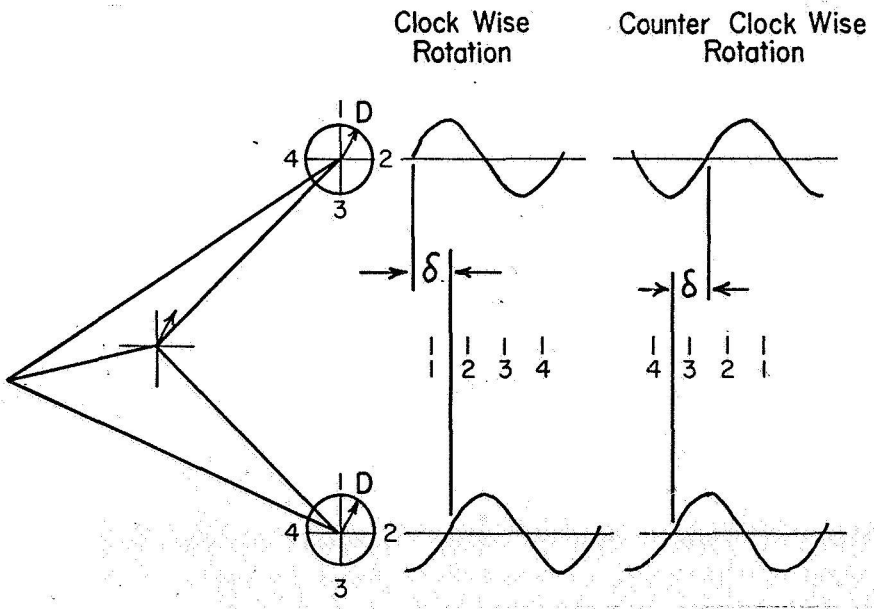

Figure 7. Rotation of Doppler signal on "stationary" carrier components. The detected components are sketched for positive, clockwise, frequency shifts. The lead-lag relationship of the two signals reverses when rotation reverses.

In similar manner:

$$3 \qquad V_b = G\cos(\omega_c t - \gamma) + D\cos(\omega_c + \omega_d)t$$

Squaring and retaining only the difference frequency terms:

$$4 \qquad V_1 = FD\cos(\omega_d t \pm \beta) \left\{\begin{matrix}\omega < 0 \\ > 0\end{matrix}\right\}$$

$$5 \qquad V_2 = GD\cos(\omega_c t \pm \gamma) \left\{\begin{matrix}\omega < 0 \\ > 0\end{matrix}\right\}$$

Phase angle δ between the detector outputs V_1 and V_2 is

$$6 \qquad \delta = \pm(\beta + \gamma) \left\{\begin{matrix}\omega < 0 \\ > 0\end{matrix}\right\}$$

The sign of the phase shift δ is thus the sign of the Doppler shift ω_d and can be used as a means of identifying flow direction. Figure 7 is a graphical and perhaps more meaningful approach to the above equations. The Doppler shifted component is shown as a phasor rotating at W_d relative to the "stationary" carrier components.

The demodulation circuit, Figure 8, is a straight forward implementation of equations 2 through 6. The only additional component is a low noise R.F. amplifier placed ahead of the mixer to improve the system noise figure. Amplifier voltage gain is intentionally small ($\simeq 10$) to avoid distortion and production of image sidebands by the large carrier component. The gain is also limited by the requirement that;

$$|V_c| < |2V_A|$$

The amplified Doppler signal and the carrier components are combined in self biasing collector detectors. A series RC phase shift

network introduces a 90° phase difference between the carrier component supplied to each detector. Operation in the square law region of Q_3 and Q_4 produces mixing of the emitter-base voltage $(\overline{V}_D + \overline{V}_A)$. Proper bias is maintained by feedback of the detected voltage appearing across R_1 C_1. The collector circuit is R.F. bypassed, allowing only the difference or Doppler shifted component to appear at the output. Low frequency transients that occur in transcutaneous applications are blocked by saturation of a saturatable inductor. A conversion gain of 15 is realized. Typical detector outputs are in the order 5mv RMS. Broadband noise output is less than 1 mv RMS.

An audio amplifier, figure 9, increases the output of each detector for monitoring and signal processing. Blocking on transients is avoided by not using emitter bypass capacitors. The emitter follower output provides a low impedance output as well as maintaining proper bias conditions in the voltage gain stage. The output at this point is 150 mv RMS signal with less than 3 mv RMS noise. Output distortion begins to occur at 1 V RMS.

Figure 8. Demodulator Circuit. A tuned input amplifier amplifies the received signal prior to addition of the carrier component added at the base of Q_3. The combined signals are detected by collector detection in Q_3. Operation in the square-law region is maintained by the bias voltage developed across R.C.

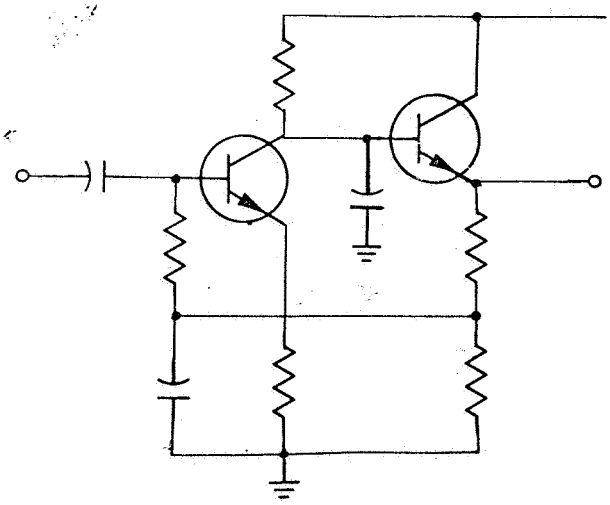

Figure 9. Audio amplifier circuit used to amplify detected signals prior to zero crossing detection. Emitter bypassing is not used to prevent distortion and latching up on transients. Band pass is flat to 20 KHz.

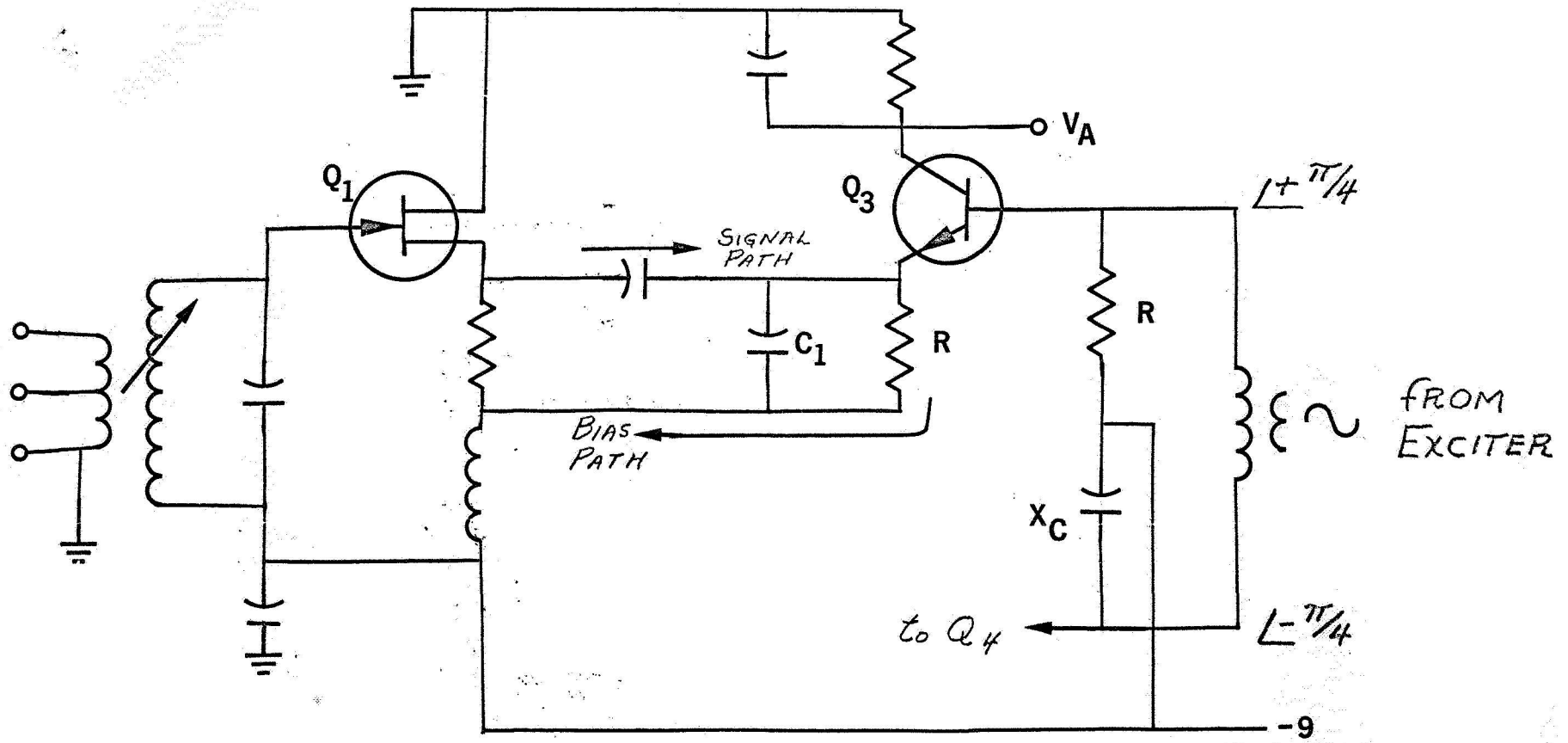

R.F. AMPLIFIER DEMODULATOR Φ SHIFT

SIGNAL PROCESSING

Mean flow velocity is empirically determined as the mean zero-crossing rate of the Doppler shifted power spectrum. The zero crossing technique, initially selected for its simplicity, has proven reliable and adequate as evidenced by the instrument's linear calibration characteristic, in figure 10. The method is further supported by the observed Gaussian relationship between the mean zero crossing rate and (S/H) the ratio of Doppler signal strength to zero crossing hysteresis. As shown in figure 11, very little change in calibration is observed over a broad range of Doppler signal amplitude.

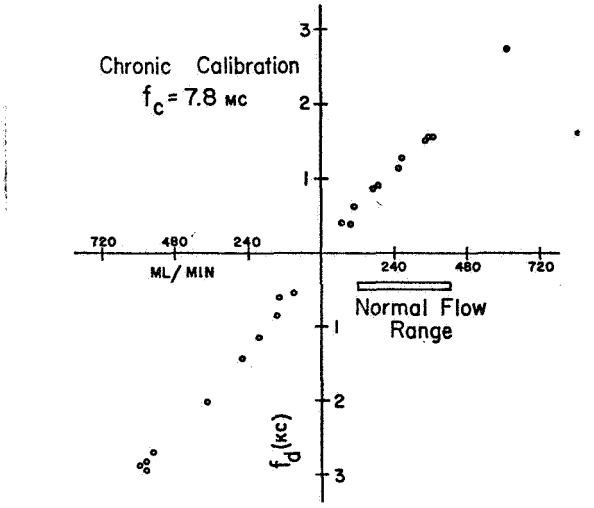

Figure 10. Chronic calibration study conducted to test use of zero crossing rate for determination of mean Doppler shift.

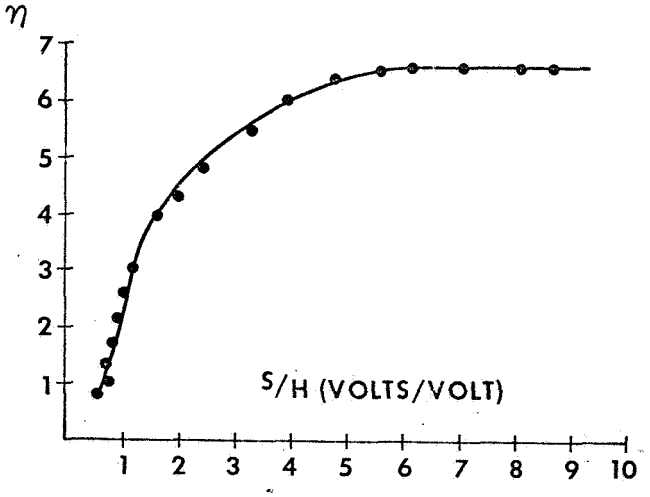

Figure 11. Relationship of calibration factor η an Schmitt trigger hystersis H. Little change in η is observed for S/H values greater than 5.

CIRCUITRY

Schmitt triggers, Figure 12, are used to detect zero crossings of the demodulated signals V_A and V_B. An operational amplifier (1/2 MC1437L) connected in a positive feedback loop is used as a low hysteresis Schmitt Trigger. The hysteresis, determined by feedback resistors R_1 and R_2, is set just above the noise level Vn, Experience has shown Vn to be nearly constant thereby allowing a fixed hysteresis. Two integrated circuit NOR gates connected as a one-shot multivibrator generate a 10 μsec. pulse for each zero-crossing. The zero-crossing sequence of V_A and V_B gates the pulse generators and thus associates the pulse with a positive or negative Doppler shift. The gated pulses are inverted, converted into current pulses, and averaged in an RC low-pass filter to obtain a voltage output proportional to the mean zero-crossing rate. Output frequency response, typically 10 m-sec., is determined by the RC time constant of the filter.

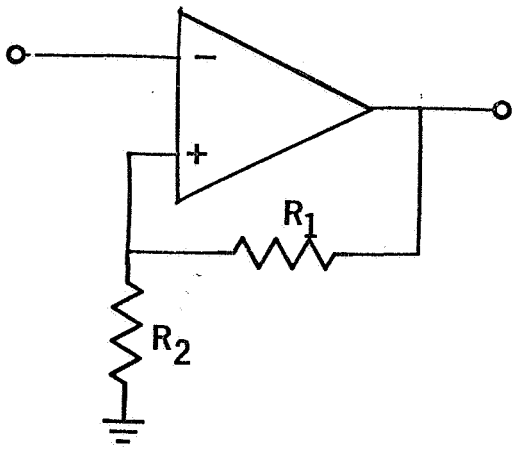

Figure 12. Highgain operational amplifiers connected in a positive feedback configuration are used as low hystersis Schmitt triggers. Hystersis H is determined by the feedback resistor ratio.

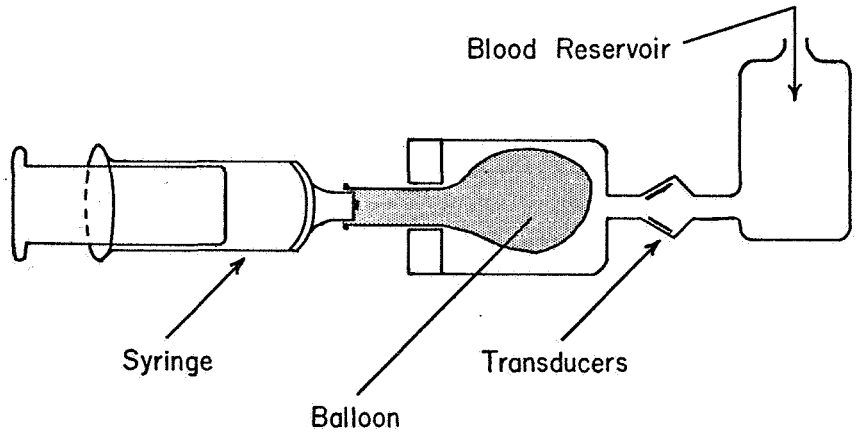

Figure 13. Flow test system. A hydralic transfer chamber is used to minimize blood cell damage and prevent introduction of bubbles into blood.

CALIBRATION PROCEDURE

Probes are calibrated and linearity characteristics determined by infusion and withdrawal of a known blood volume at different rates. A closed flow system, figure 13, is used to prevent inadvertent introduction and production of bubbles. The comparatively large scattering crossection of bubbles gives rise to large Doppler signals which interfer with the calibration procedure. A rubber diaphragm is used to isolate the displacement piston from the blood and thus prevent both jamming of the piston and cell damage. During studies sterile saline is used as a transfer fluid between the piston and diaphragm in the event of a diaphragm failure. The piston is either hand operated or driven with a cam to produce a sine-wave flow.

Heat shrink tubing is generally used as an artifical artery. It is innert and easily shrunk to fit the probe being tested. Arterial constrictions and obstructions are easily simulated by heating and deforming the tubing. Following the experiment, a cast of the flow section is made by filling the section with epoxy or dental resin. The tubing is slit and removed leaving a cast from which the internal cross-section is easily determined.

Prior to use the entire system is throughly cleaned and flushed with a sterile-isotonic saline to remove foreign particles and prevent hemolysis. A small amount of heperin is added to prevent clot formation. Constant cycling for a period of 1 to 2 hours is required to flush all bubbles from the system. This time is reduced by careful cleaning of the system and pouring of the blood.

DATA PRESENTATION

Non-linearities and zero offsets are not easily recognized when calibration data is presented in the conventional form:

$$\text{output} = F(V)$$

Such a graph tends to mask and hide the very information the calibration test is intended to provide. A graph of the area under the deflection generated by a standard volume flow plotted as a function of the infusion time is easily plotted from raw data and tends to maximize the desired information.

$$\int_{T} (\text{Output})\, dt = F(T)$$

On such a graph, a zero offset appears as the slope of a line and a non-linearity as a break in the line. A set of typical data is presented in both forms, in figure 14 a and b. The sharp break in the curve was introduced by band limiting the audio band pass with a 10 KC low pass filter.

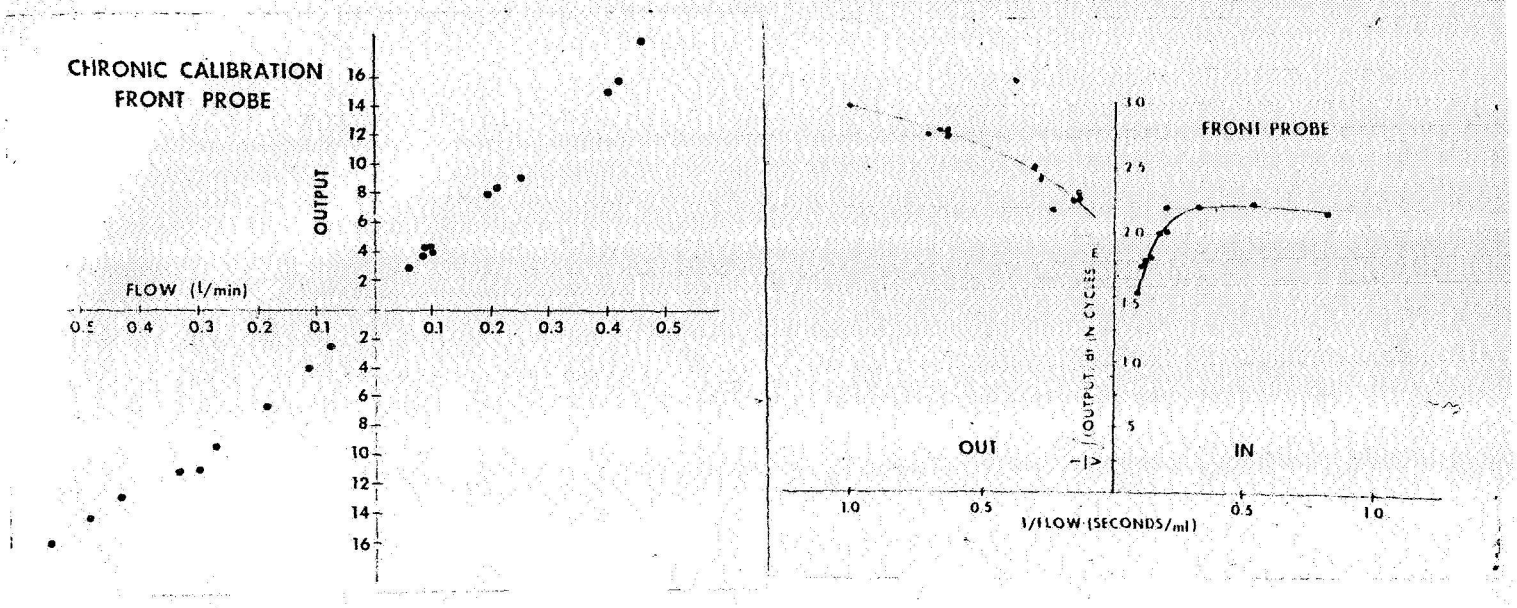

Figure 14. Presentation of calibration data. The plot, reveals non-linearities hidden in conventional plot of the same data.

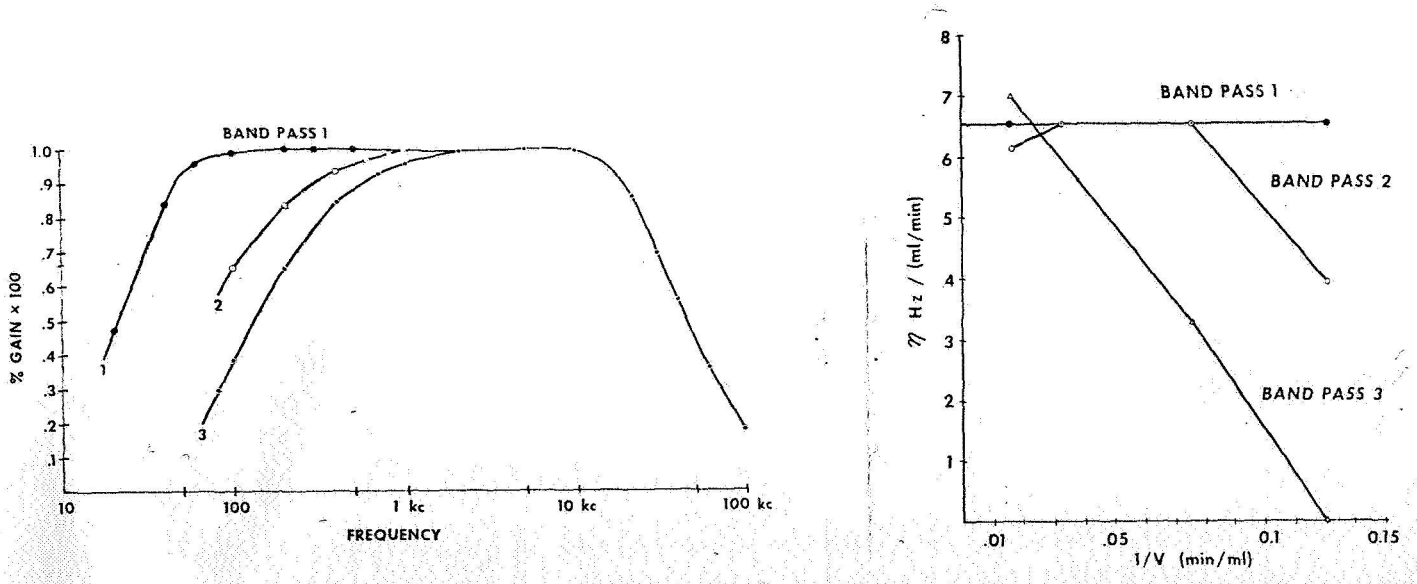

Figure 15a. A zero offset produced by band limiting low frequency components. A single stage RC coupling network was used to limit the low frequency shifts b. Corresponding band pass characteristics used in the above test. The .1 μf capacitor and inductor combination is normally used for transcutaneous applications.

CALIBRATION RESULTS

Bench calibrations were conducted as an overall test of instrument performance and to evaluate assumptions made during the design process. Under conditions of laminar non-turbulent flow a linear response characteristic is observed. This response characteristic or calibration curve is, however, subject to operating conditions signal-to-noise ratio, signal to zero-crossing hysteresis ratio, system bandpass characteristics and under conditions of pulsitale flow; probe design. Signal-to-noise ratio, the parameter most subject to operating conditions, influences sensitivity and can under extreme cases completely obliterate the flow signal. In addition to calibration changes, S/N is seen to affect the clarity of the output signal. A family of sine-wave tests, Figure 14, shows both the reduction in output clarity and change in sensitivity. Generally speaking a S/N ratio of (20) dB is required for good signal clarity while only a (2) dB S/N ratio is required for mean flow measurement. The relationship of the output time constant to signal clarity has not yet been quantitatively observed. Typical signal levels and S/N ratios ranging from 32 dB on the digital artery to 60 dB on a cartoid implant are tabulated in Table 1.

A family of calibration curves, Figure 15, illustrates, the zero offset produced by altering the low frequency response of the audio amplifier used to amplify the demodulated signal prior to signal processing. The low frequency response is that of a single stage RC filter. Ideally a DC or near DC response is desired, this however is not practical because the low frequency artifacts of artery wall motion, probe and probe lead

TABLE I

TYPICAL SIGNAL LEVELS

fo = 9.0 MHz

V_e = 1.0 VRMS

Noise (Referred to output 1 mv RMS)

LOCATION	SIGNAL OUTPUT	SIGNAL INPUT		S/N
Digital Artery	80	20	-94	38
Radial Artery	130	33	-90	42
Radial Vein	250	62	-84	48
Cartoid Artery (Implant sheep)	250	62	-84	48
Units	MV RMS	VRMS	db. $20 \log \frac{Vin}{Ve}$	db

motion if not eliminated tend to interfere with the zero-crossing signal processing. A time constant of .01 seconds seem to represent a satisfactory compromise between zero offset and practical operation. A 20 henry saturatable choke is added to the filter network for transcutaneous operation to filter out the large flow frequency transients associated with motion of the probe relative to the vessel wall and other underlying bone and tissue structures. The high frequency response is limited to 15 KHz by two independent RC filters to both reduce noise and provide a symmetrical noise spectrum. An asymmetrical or skewed noise spectrum will provide a zero-offset as well as alter the calibration. Studies of this effect have been limited to quantitative observation.

The relationship between calibration, η, and S/H, the signal-to-hysteresis ratio is a means of demonstrating the Gaussian statistics of the Doppler signal (Fig. 11). Less than 5 percent change in η is observed for S/H ratios greater than (14) dB, allowing the hystersis to be fixed at a level just above the incoming noise level.

A transducer consisting of two 4.8 mm dia LTZ-5 mounted at a 50° angle from the flow axis was used during the calibration studies. When used with a 0.22" dia flow section a 6.55 Hz/ml/min calibration factor is observed. This is to be compared with a predicted value of 4.69 Hz/ml/min. The 1.4 ratio between predicted or observed values suggest that the probe is sensing the center or peak velocities of a parabolic velocity profile. The ratio of peak to average velocity in a parabolic profile is 1.5. Beam visualization with a Schelern system confirms that

the transducer radiation pattern is indeed limited to the center of the test section. The hypothesis is further supported by the relatively narrow spread in frequency shifts revealed by spectral analysis.

Turbulent flow produced by a tight fitting probe produced changes in the calibration factor. Such implants are characterized by non-linear and asymnetrical calibration curves. Two tight fitting probes were implanted adjacent to each other in an effort to establish the cause of the observed nonlinearity. The curves, Fig. 16a and b, represent mirror images suggesting that the "jet" produced by the upstream probe constriction was affecting the calibration factor and that the probes are indeed profile sensitive. A more complete understanding of the interlationship between flow profile and calibration is required for quantitative flow measurements. These nonlinearities are not seen with catheter probes and properly fitted probes.

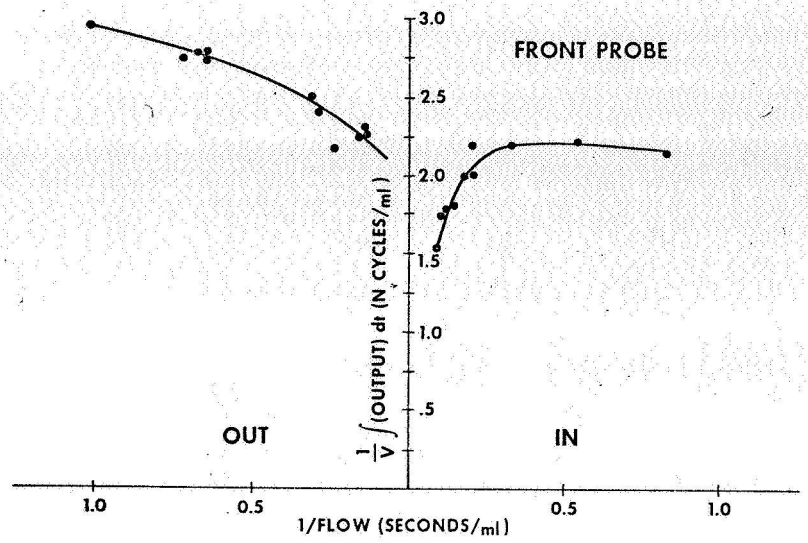

Figure 16 a and b. Calibration of tight fit adjacent implanted probes. Constriction caused by probe produces a jet affecting the linearity of the down stream probe.

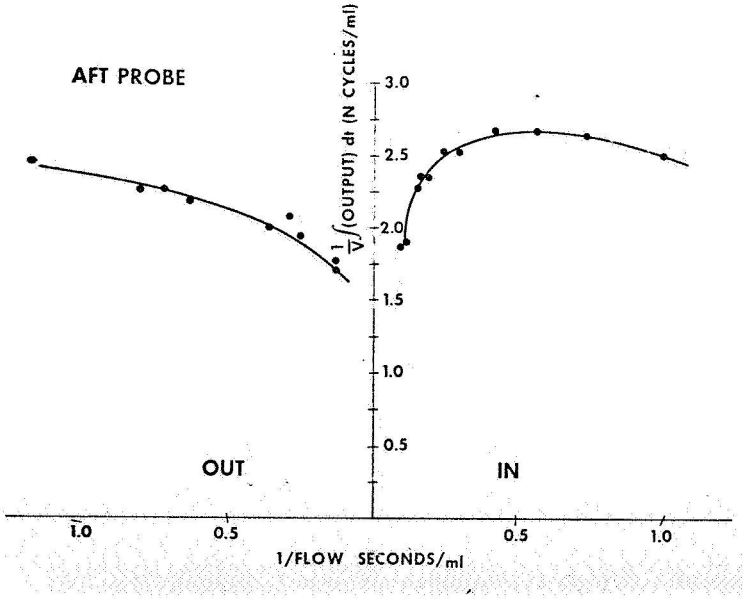

CONCLUSIONS

The electronic package developed has proven reliable as well as simple to operate. Power consumption of the exciter-demodulator is small ($\simeq$ 100 mw), making the method adaptable for telemetry applications. Reproducability in all tests has been better than 5%. Signal-to-noise ratios range from 30dB during trancutaneous observation of digital artery to 50 dB on a cartoid artery implant. Zero resolution is better than $\pm$ 5 ml/min. Linearity in laminar flow range is better than 1%. However; linearity is severly degraded in the transition from laminar to blunt flow. Improvement in this parameter will hopefully result from a more complete understanding of transducer radiation patterns and subsequent advances in probe design.

REFERENCES

1. O'Rourke, "Pressure and flow waves in systemic arteries." Journal of Applied Physiology, Vol. 23, No. 2, August 1967.

2. Franklin, Schlegel, and Rushmer, "Blood flow measured by Doppler frequency shift of back scattered ultra sound." Science 134: 564, 1961.

3. Rushmer, R. F., Baker, D. W. and Stegall, H. F., "Transcutaneous Doppler flow detection as a non-destructive technique. J. Appl. Physiology 21: 554-566, 1966.

4. Norgaard, D. E., "The phase shift method of single sideband generation:, Proc IRE, Vo. 44, No. 12, p. 1718, December, 1956.

5. Ekstrom, P. A., "Distinguishing between positive and negative difference frequencies." Review of Scientific Instruments. Vol. 37, No. 9, p. 1244-1245. 1966.

6. McLeod, F. D., Jr. "A directional Doppler flowmeter. Digest of 7th Internation Conference on Medical and Biological Engineering. Stockholm, p. 213, 1967.

APPENDIX I

SCHEMATIC DIAGRAMS

and

PARTS LIST

APPENDIX II

RELATED PATENT

DISCLOSURE

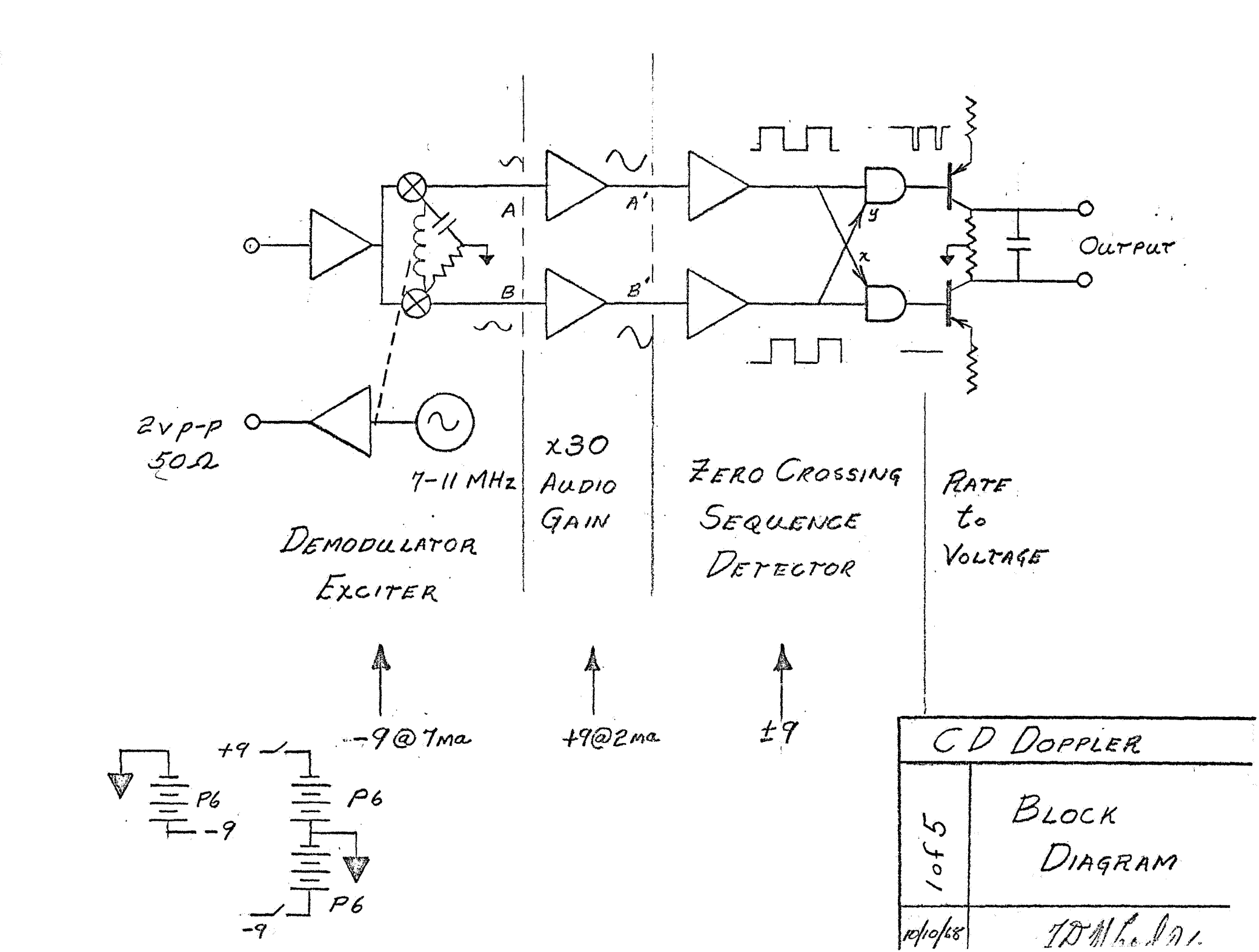

CD Doppler	
1 of 5	Block Diagram
10/10/68	TDM Co. Div.

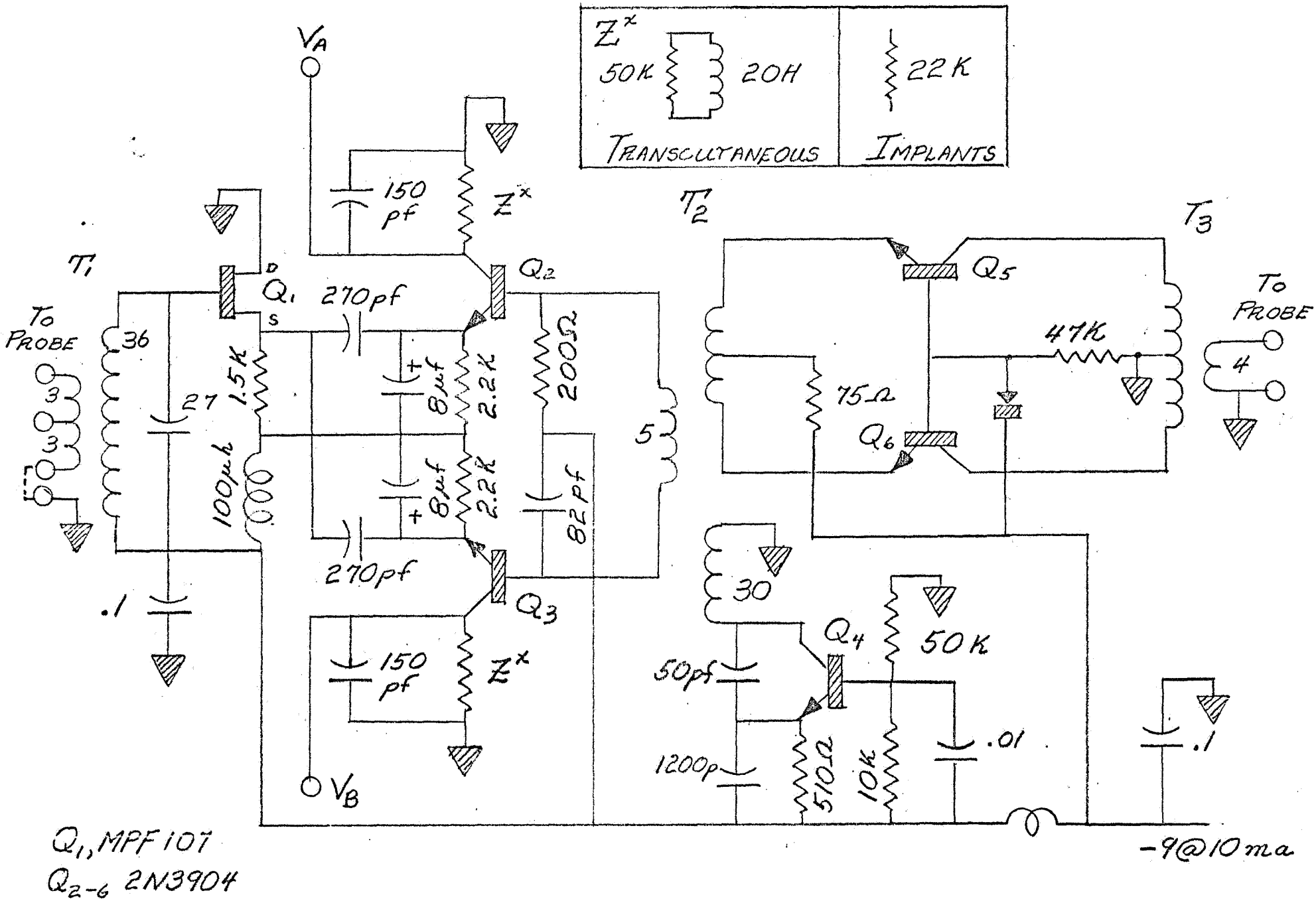
Zx
50K
20H
TRANSCUTANEOUS
22K
IMPLANTS
VA
150 pf
Zx
T1
T2
T3
Q1
Q2
Q3
Q4
Q5
Q6
D
S
270pf
To PROBE
36
3
3
27
100µh
1.5K
8µf
2.2K
8µf
2.2K
200Ω
82pf
5
270pf
.1
150 pf
Zx
VB
75Ω
47K
4
30
50pf
1200p
50K
510Ω
10K
.01
.1
-9@10ma
Q1, MPF107
Q2-6 2N3904

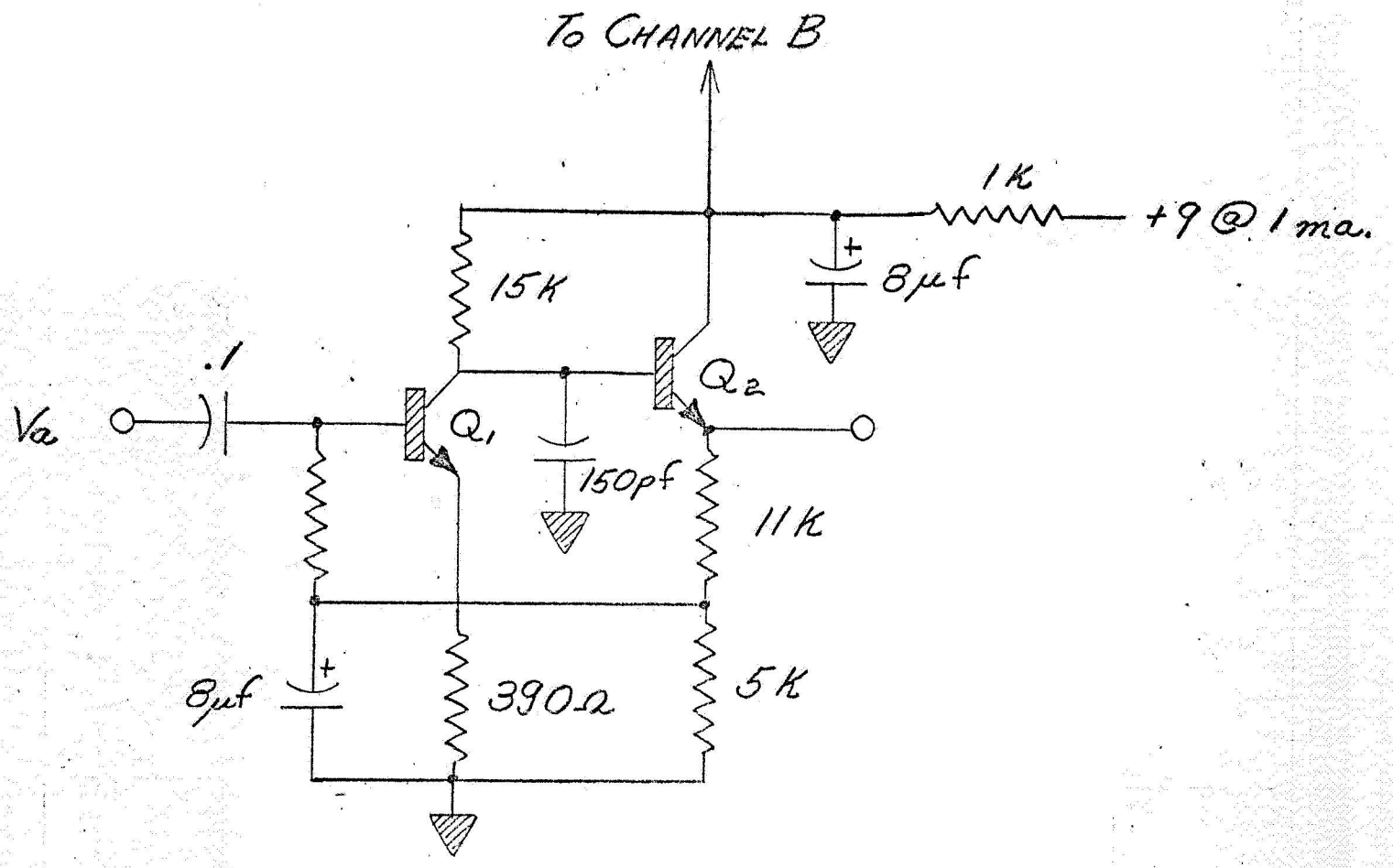

Gain: x30

Bandpass: 20cps → 15Kc

C D Doppler	
	Audio Amplifier
	4 9 of 1.

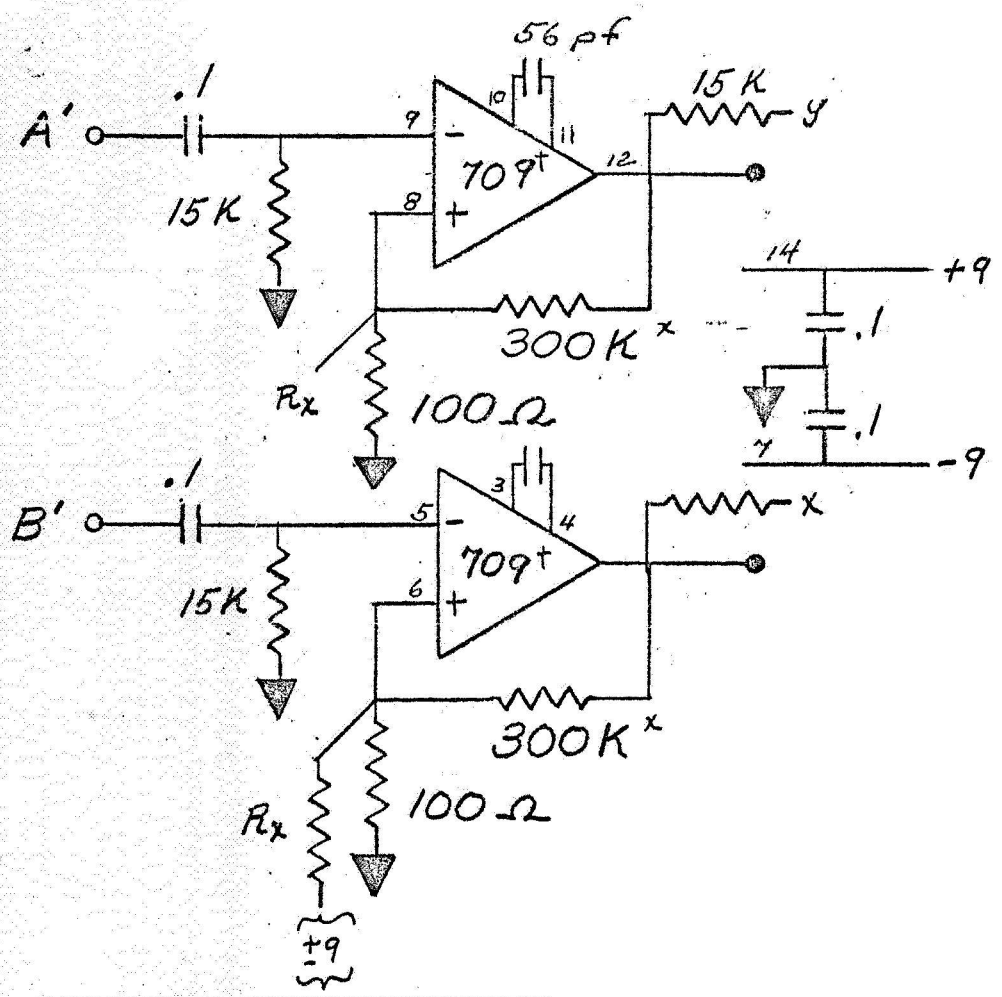

R_x 100K → 2MEG BAL
x SOME 709 REQUIRE 100 pf SHUNT
† ½ DUAL 709 MC 1437

HYSTERSIS : ≈ 6 MV
SUPPLY +9, -9

C-D DOPPLER	
5 of 4	SCHMITT TRIGGER
10/14/68	JD M Lewis

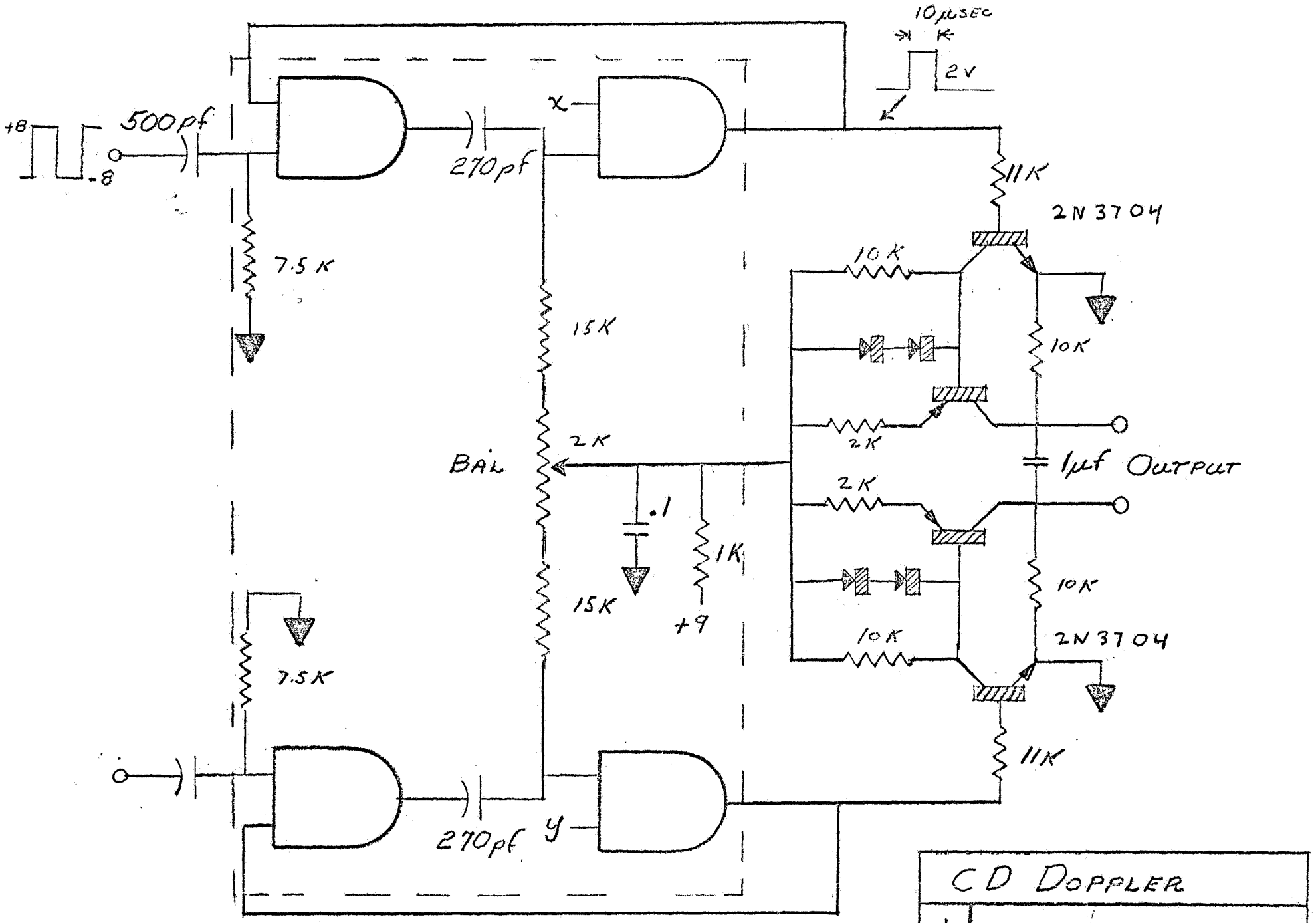

CD DOPPLER

5 of 5

GATED ONE SHOTS

PARTS LIST

EXCITER DEMODULATOR

Resistors, 1/4 watt, 5%

Value	Quantity
51 Ω	1
200 Ω	1
510 Ω	1
1.5 K	1
2.2 K	2
10 K	1
47 K	2
51 K	2

CAPACITORS

			Quantity
12 PF, 27, 56, SIVMIC			1
100 PF	1 KV Disc	.250 Lead Spacing	1
150 PF	1 KV Disc	.250 Lead Spacing	2
270 PF	1 KV Disc	.250 Lead Spacing	2
1200	1 KV Disc	.250 Lead Spacing	1
.01	1 KV Disc	.250 Lead Spacing	1
.1	25 V Disc	.400 Lead Spacing	4
8.0	15 V Elec	.110 Diam .300 LG.	1
2-56	pf		

INDUCTORS

100	.100 diam.	.250 lg	2 ea.
UTC	DO T 49	Series Wire D	2 ea.
Micrometals	L56-6 -CT-B-6		1 ea.
	L 56-2-CT-B-6		1 ea.
TRANSISTORS	2N3904		6 ea.
	MpF 107		1 ea.

PARTS LIST

SIGNAL PROCESSOR

RESISTORS
1 1/4 Watt 5%

Value	Quantity
100	2
290	2
1 K	1
1.5 K	1
2 K	2
5.1 K	2
7.5 K	2
10 K	4
11 K	4
15 K	8
68 K	2
200 K	2

Trimpot 2K Mod. 3282W 1 ea.

CAPACITORS

100 PF	1 KV Disc	.250	Lead Spacing	2
150 PF	1 KV Disc	.250	Lead Spacing	2
250 PF	1 KV Disc	.250	Lead Spacing	2
500 PF	1 KV Disc	.250	Lead Spacing	2
.01	1 KV Disc	.250	Lead Spacing	2
.1	25 V Disc	.400	Lead Spacing	7
8.0	15 V Elec	.110	Diam .300 LG	3
20	15 V Elec	.110	Diam. 450 LG	1

2N 3904 10 ea.
2N 3906 2 ea.
MC 817 p 1 ea.
MC 1437L 1 ea.

Jack Switchcraft	TR -2A-p2	2 ea.
1 C Socket Barnes	041-001-111	2 ea.

A PRELIMINARY PATENT DISCLOSURE

Made

to

National Aeronautics

and

Space Administration

by

F. D. McLeod

on

Work supported and conducted

under NASA Grant

This disclosure relates a method for reducing interference in Doppler effect flowmeters. A hybrid coil arrangement is used to reduce exciter noise, R.F. interference from external sources and the artifact signal produced by vessel wall motion.

Method

Two transducer elements, mounted so as to provide overlapping radiation patterns, are connected to a balanced input as shown in Figure 1. Exciter power, (10Mhz) provided to the center-tap, divides equally between the transducer elements. The amount of exciter voltage induced in the primary of T_1 is determined by the matching of the transducer elements. Waves reflected from large tissue interfaces appear equally at the transducer elements and are rejected as common mode signals. Similarly, interference from external R.F. sources is equally coupled into the transducer elements and is also rejected as common mode.

Discussion

A. Suppression of Direct Coupled Carrier

Leakage between conventionally connected exciter and demodulator transducer elements is typically as high as 10% of the exciter voltage. Thus, any improvement requires better than 10% matching of the transducer elements. An adjustable balance circuit is shown in Figure 2. The differential capacitor permits complete suppression of the carrier. This, however, represents another panel control. A significant advantage is realized with catheter probes where it is difficult to shield the exciter and demodulator leads. A shielded pair can be substituted for the present double coax.

B. Reduction of Reflection from Large Reflectors

Reduction of signals from large reflectors as vessel walls depends to a large degree on the alignment of the transducer radiation patterns. This is difficult to attain with the present adjacent placement of transducer elements. The use of transducer arrays is though to be a solution to this problem. A marked reduction in wall motion has been seen with catheters. No major improvement with transcutaneous probes has been realized.

C. Suppression of External Interference

Interference from external R.F. sources is reduced by over 20 Db. and does not require careful watching of the transducer elements. This could represent a critical improvement on flowmeters operated in the presence of R.F. fields and other R.F. equipment.

Summary

This disclosure relates application of the hybrid coil to the Doppler flowmeter. The desired reduction in vessel wall motion artifact has not been fully realized. Reduced shielding requirements between exciter and demodulator leads simplified construction of small catheter probes.

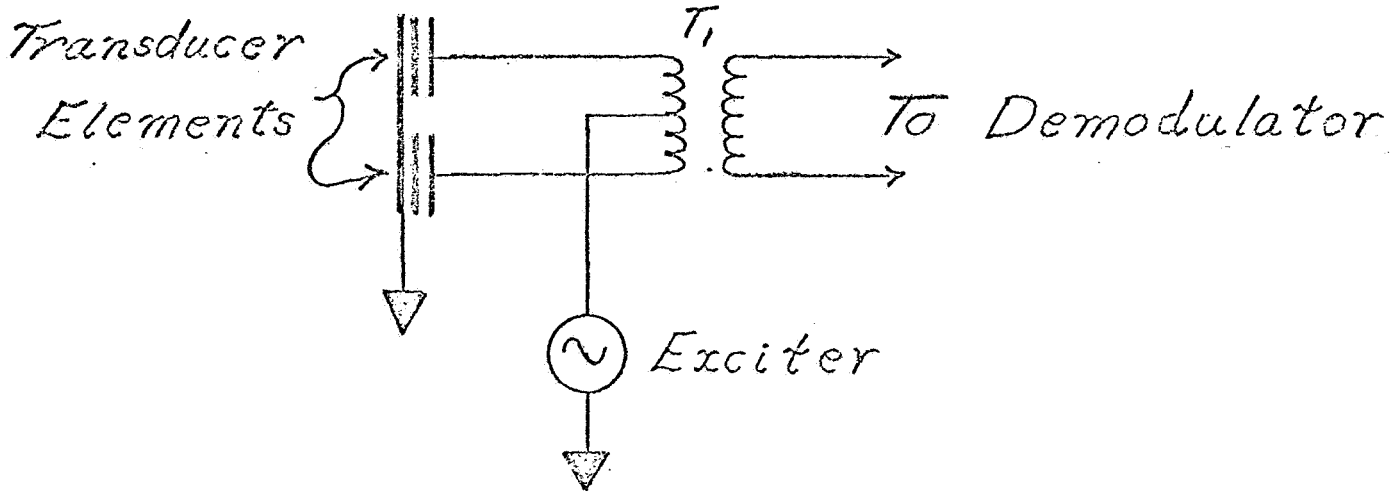

Fig. 1

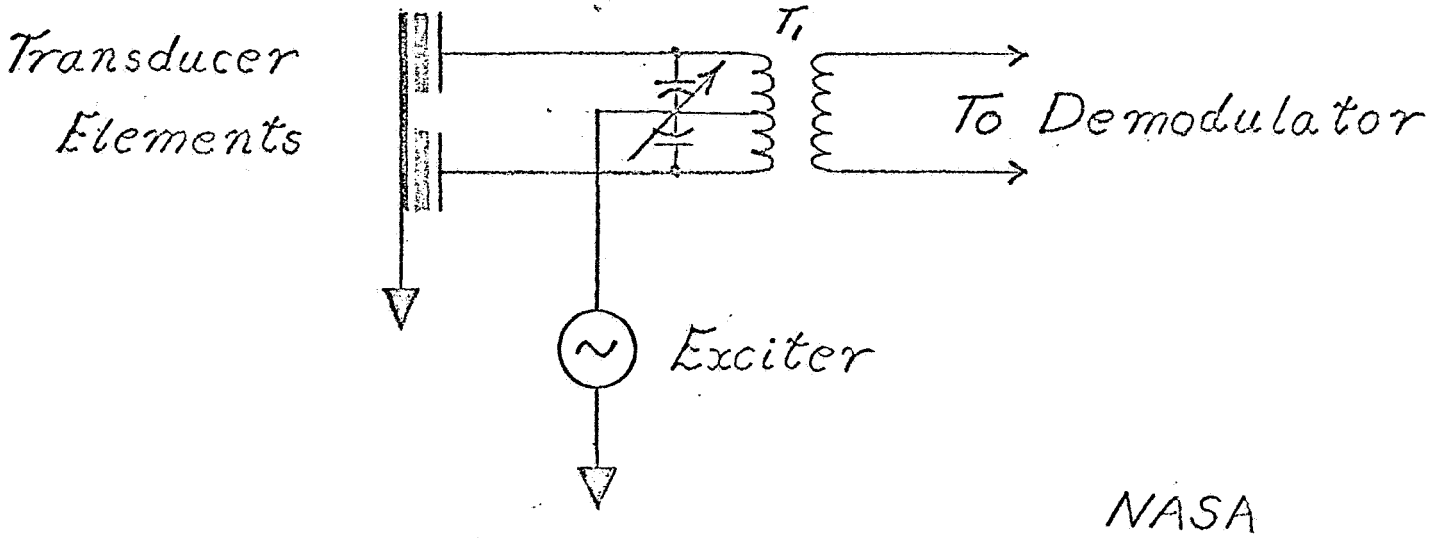

Fig 2

NASA
McLEOD